MECHANIKA TEORETYCZNA
I STOSOWANA
Journal of Theoretical
and Applied Mechanics
4, 33, 1995

CALCULATION OF THE WING AERODYNAMIC CHARACTERISTICS WITH GROUND EFFECT USING PANEL METHODS[1]

JANUSZ SZNAJDER

ZDOBYSŁAW GORAJ

Institute of Aviation, Warsaw

This paper presents a mathematical model of the flow around wings near the ground. A potential flow was assumed in the whole domain, excluding vortex wake. Two calculational models are considered: the first one, for thin wings, based on the vortex lattice method, and the second one, for thick wings, based on the Hess method.
The aerodynamic characteristics calculated are: lift coefficient, pitching moment coefficient, induced drag coefficient and also the gradient of lift coefficient and the induced angle of attack as a function of the altitude above the ground.
There is presented a comparison between the aerodynamic characteristics calculated assuming infinitesimaly thin wing and those calculated using the method including the wing thickness.

List of symbols

b	–	wing span
c	–	wing chord
c_l	–	lift coefficient
c_m	–	pitching moment coefficient
c_{di}	–	induced drag coefficient
L	–	lift force
h	–	altitude above the ground
Ma	–	Mach number
$\boldsymbol{Q}_\infty$	–	free stream velocity vector
α	–	angle of attack

[1]Presented in VI-th Conference "Mechanics in Aviation", Warszawa, May 1994

$\boldsymbol{\Gamma}_i$	–	circulation vector
ρ	–	air density
VLM	–	vortex lattice method
TWM	–	thick wing method

1. Introduction

Aerodynamic characteristics of the airplane near ground change as a result of disturbances in the flow caused by the presence of ground. These changes become significant when the altitude is less than the wing span. The most important changes in aerodynamic characteristics are as follows:

1. Reduction in the induced drag as due to the induced downwash decreasing
2. Increase in the lift coefficient gradient due to pressure increment under the wing, caused by the increase in the local angle of attack
3. Reduction of the critical angle of attack and $c_{l\max}$ due to flow separation, particularly for the configuration with flaps on.

For the ground effect analysis, a "mirror image" method has been chosen. This method consists in placing two wings in the test section of wing tunnel. These wings are geometrically identical and are placed in such a way that they are arranged symmetrically with respect to ficticious ground.

The flow around such configuration of wings was calculated by means of the panel methods. Two different models were used: the first one, based on the vortex lattice method (VLM), and the second one, for thick wings (TWM), assuming the source and vorticity distributions on the wing chord plane.

Because of the fact, that the model does not introduce the flow separations, the paper is focused on the phenomena described in points 1 and 2.

The main object for using these two models was to analyze the differences among the calculated characteristics of wings with the ground effect, appearing due to neglecting the wing thickness in the VLM, since the methods based on the VLM are widely used in the analysis of the flow around wings, including the ground effect.

The ground effect has been investigated since the 1920-ies, but for most of the time, there has been no simple calculation method, which would be applicable to wings of arbitrary configuration. The methods in use were based on the assumption that the wing could be modeled by a single vortex of intensity varying over the span, and were more or less simplified depending on whether one did or did not take into account the effect of bound vorticity of the "image" wing on the "real" wing. The development of panel methods (cf Hedman (1965); Hess and Smith (1966); Maskew and Woodward (1976); Singh et al. (1983); Bertin and Smith (1989); Katz and Plotkin (1991)) has provided the efficient tool for analysis of the flow around arbitrary configurations including the mentioned above and previously neglected flow phenomena. In recent investigations new, important phenomena were included into analysis, namely, the behavior of the vortex wakes released near the ground by large aircraft and its impact on smaller aircraft (cf Liu et al. (1992)). However, in many publications, e.g., Lan (1976), the wing thickness is reduced to zero, or it is assumed that the wing is thin, so it is interesting to compare the results of method which makes no limitations regarding the wing thickness with the results of the method assuming ifinitesimaly thin wing.

2. Mathematical model

It is assumed that the flow is steady, incompressible, inviscid and irrotational (excluding the flow inside infinitesimaly thin wake where the flow is rotational). The angles of attack and perturbations are assumed to be small, so the potential of flow exists in the following form

$$\phi = \phi_\infty + \varphi \tag{2.1}$$

where
ϕ_∞ – potential of the free stream
φ – potential of the disturbances in the flow.

The governing Prandtl-Glauert equation has the form

$$(1 - \mathrm{Ma}^2)\phi_{xx} + \phi_{yy} + \phi_{zz} = 0 \tag{2.2}$$

and can be transformed into the Laplace equation

$$\phi_{xx} + \phi_{yy} + \phi_{zz} = 0 \tag{2.3}$$

The boundary conditions are

- at infinity $\mathrm{grad}\varphi \rightarrow 0$
- at the control points of wing surface $d\phi/d\boldsymbol{n} = 0$

This leads to the following set of linear equations

$$\mathsf{A}X = -\{Q_\infty \boldsymbol{n}_i\} \tag{2.4}$$

where

A – matrix of the influence coefficients containing velocities due to singularities of unit strength placed on surface elements (panels) of the wing. The nth row of the matrix contains velocities induced by the singularities of all panels the nth control point

$\boldsymbol{X}$ – vector of the unknown strength of the singularities

$\boldsymbol{n}_i$ – normal vector at the control points.

The local angle of attack is modeled by deflection of the normal vector at the control points by an angle equal to the local surface slope of the mean camber line. This has been shown by Lan (1976) to give correct results for the values of the angle of attack up to 10 degrees.

The vortex lattice method (VLM) (cf Hedman (1965); Bertin and Smith (1989); Katz and Plotkin (1991)) assumes the horseshoe vortices on each panel surface. The horseshoe vortex is composed of the bound vortex line, laying span-wise on the panel surface and of two free vortex lines, of the same strength as the bound vortex, stretching to infinity behind the wing. Velocities induced by the vortex system at the point P of the flow field are obtained using the Biot-Savart law (Fig.1)

$$\boldsymbol{V} = \frac{\Gamma}{4\pi}\frac{\boldsymbol{r}_1 \times \boldsymbol{r}_2}{|\boldsymbol{r}_1 \times \boldsymbol{r}_2|^2}\Big[\boldsymbol{r}_0\Big(\frac{\boldsymbol{r}_1}{r_1} - \frac{\boldsymbol{r}_2}{r_2}\Big)\Big] \tag{2.5}$$

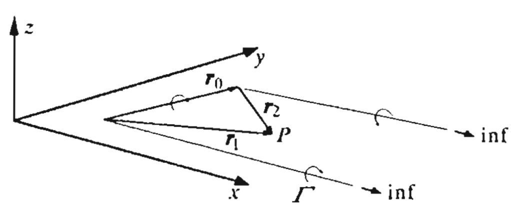

Fig. 1. Calculation of the velocities induced by a horseshoe vortex

In the method for thick wings (cf Singh et al. (1983)) the surface vorticity and source distribution is assumed on the chord plane of the wing. The

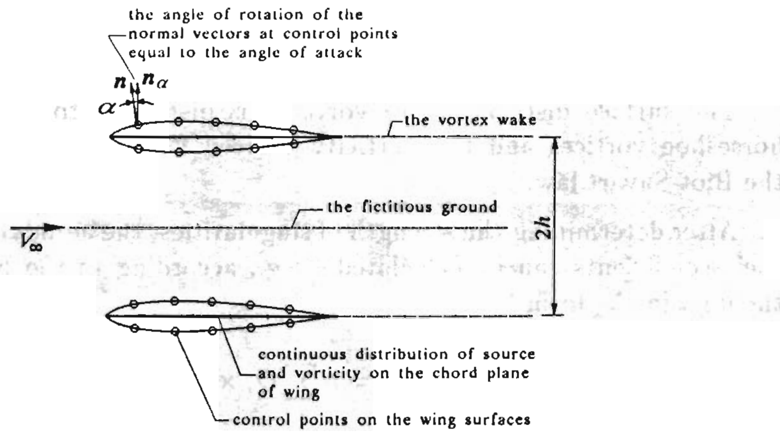

Fig. 3. Modelling of the geometry of thick wings near the ground

3. Results

Fig.4 and Fig.5 show the results obtained for a two dimensional flow.

Fig.4 shows the ratio $c_{lg}/c_{l\,\mathrm{inf}}$ of a wing with NACA 0010 section including the ground effect, obtained using the VLM and TWM methods, versus the relative altitude h/c.

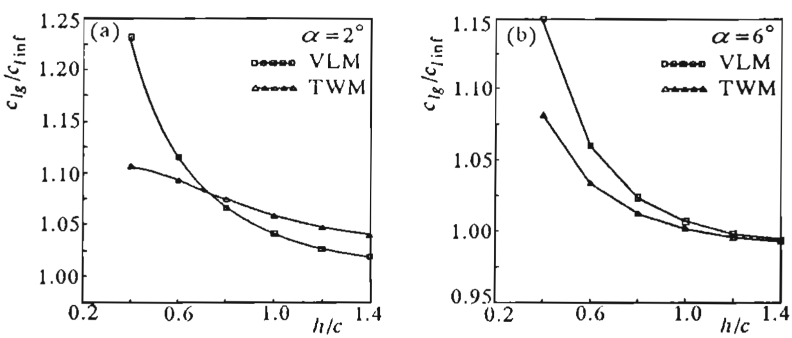

Fig. 4. The ratio $c_{lg}/c_{l\,\mathrm{inf}}$ in a two dimensional flow vs. the relative altitude

It is visible, that, for altitudes less then approximately one wing chord, the wing thickness must be taken into account in the flow analysis.

The wing thickness is responsible for inducing velocities which are neglected by methods based on the VLM, especially at small angles of attack, effects velocities due to the source distribution are calculated assuming the constant source distribution on the surface of each panel (cf Hess and Smith (1966)).

The surface distribution of vorticity is disretised to a finite number of horseshoe vortices and the vorticity-induced velocities are calculated using the Biot-Savart law.

After determining the strength of singularities, the aerodynamic forces and their coefficients can be calculated , e.g., according to the Kutta-Joukowski theorem in the form

$$F = \rho \sum_i Q_i \times \Gamma_i \qquad (2.6)$$

where Q_i are the resultant velocities at the points lying in the middle of the bound vortex lines in the case of VLM. In the TWM case the resultant velocities and pressure at the control points are calculated, and the pressure distribution is integrated over the wing surface.

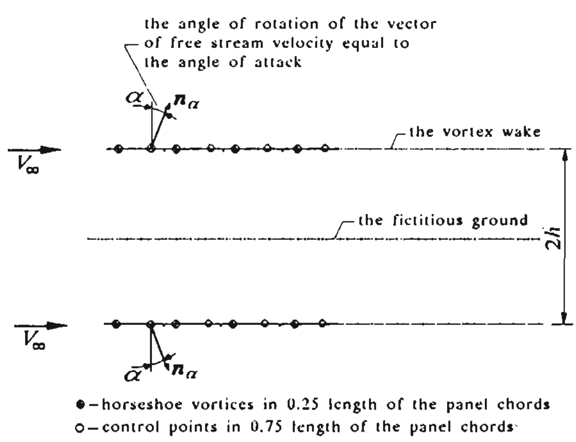

Fig. 2. Modelling of the geometry of thin wings near the ground

In both models (Fig.2 and Fig.3), the vortex wake was assumed to be planar, stretching to infinity behind the wings. The calculations were made for low speed, for which the effects of compressibility of the fluid could be neglected.

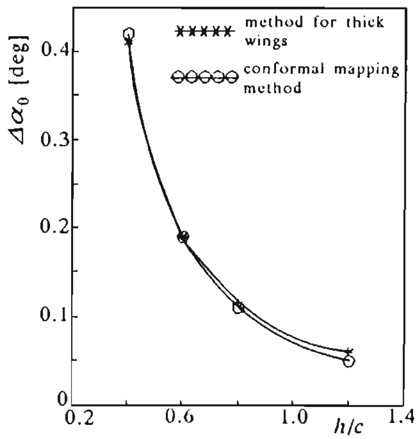

Fig. 5. The change of zero-lift angle of attack in a two dimensional flow due to the wing thickness vs. the relative altitude

of which are visible in Fig.4. An example of this may be also the change of zero-lift angle of attack, shown in Fig.5.

Calculations were made for the NACA-0010 wing section using the method for thick wings (cf Singh et al. (1983)), and are in very good agreement with the results of the conformal mapping method (after de Sievers [2]).

Fig.6 shows the ratio of the lift coefficient gradient near the ground for a wing of aspect ratio 5 having NACA-0010 section. Shown are results of both the tested methods (VLM and TWM) end experimental results (from Fiecke (1956)).

The calculational methods give here correct results for the relative altitude greater than 0.2 of the wing span.

Both methods were also applied to calculation of the increment of the induced angle of attack and pitching moment coefficient close to the ground.

The results of both tested methods were plotted against the values of the lift coefficient (Fig.7, $\Delta\alpha_{\rm ind} = \alpha_{\rm ind\ in\ ground\ effect} - \alpha_{\rm ind\ outside\ ground\ effect}$, the definition of the Δc_m is similar).

The comparison in the case of the induced angle of attack was made for two values of the relative altitude, $h/c = 1.2$ and $h/c = 0.4$. For a greater altitude, the results of the method for thick wings are in good agreement with the results of the vortex lattice method. For smaller values of the altitude, the wing thickness manifests itself in the vertical shift of the curve for thick wings.

The change of the pitching moment coefficient near the ground was cal-

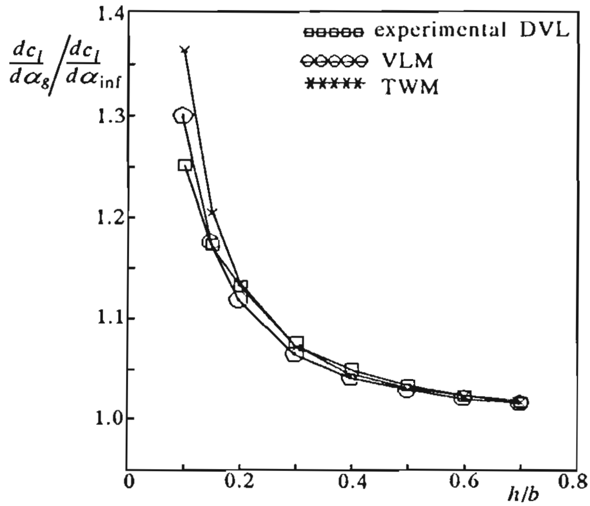

Fig. 6. The ratio of the gradient of the lift coefficient near the ground vs. the relative altitude

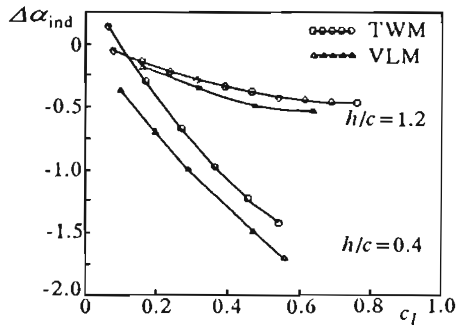

Fig. 7. The increment of the induced angle of attack close to the ground as a function of the lift coefficient

culated in a similar way. The results are shown in Fig.8. It is visible, that the wing thickness exerts even stronger influence on the change of pitching moment coefficient than on the induced angle of attack, and, particularly for the pitching moment calculations, the wing thickness can not be neglected for altitudes lower than the wing chord.

The induced drag coefficients are shown in Fig.9a,b.

In both the methods (VLM and TWM) calculations of the induced drag coefficient were made in the Trefftz plane (cf Katz and Plotkin (1991), p.233), far behind the wing. In Fig.9a coefficient k defined as $k = c_{di\,g}/(c_l^2/\pi\Lambda)$ is

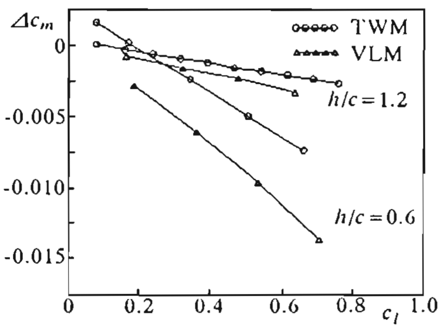

Fig. 8. The increment of the pitching moment coefficient near the ground as a function of c_l

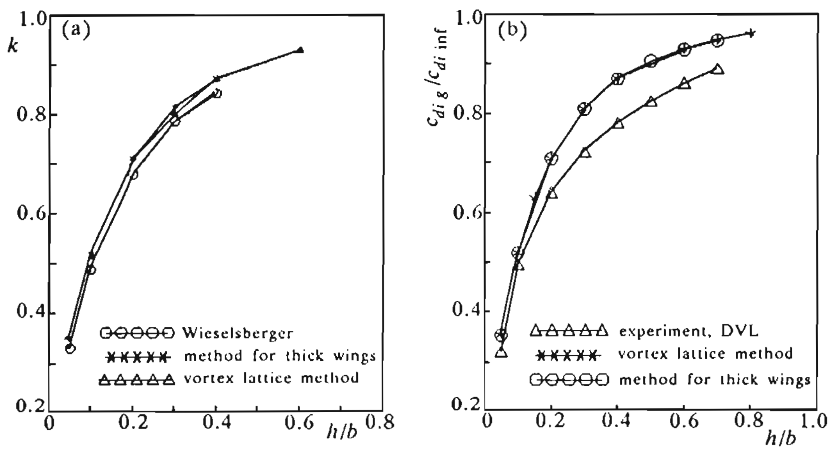

Fig. 9. (a) – The coefficient $k = c_{di\ g}/(c_l^2/\pi\Lambda)$ as a function of the relative altitude; (b) – the ratio $c_{di\ g}/c_{di\ \mathrm{inf}}$ as a function of the relative altitude

shown, where the subscript g denotes the presence of ground.

The results of both (VLM and TWM) methods are compared to the results of Wieselsberger's analytical method (cf Thwaites (1960)), which includes the effect of vortex wake of the image wing. The agreement between the results of all methods is very good in the whole range of altitudes.

Fig.9b shows the values of $c_{di\ g}/c_{di\ \infty}$ obtained using both tested methods in comparison with the experimental values. The values of the induced drag coefficient near the ground and far from the ground were obtained for the same lift coefficient. Both methods give here identical results which do not entirely agree with the experimental results. However, in spite of this, both methods do predict the phenomenon of the reduction of the induced drag by half for wing placed at an altitude of 0.1 of the wing span above the ground.

The perfect correlation between the results of TWM and VLM in the induced drag calculation may be explained by the fact, that the drag force is dependent of the value of the circulation Γ, which is responsible for the lift force. Since the calculations were made in both cases for the same lift, the drag is also the same.

The vortex wake behind wings has been assumed in the present work to be planar. In reality, since the vortex wake tendents to roll up and because of the interactions between the vortex wake of the "real" and the "image" wing, the actual shape of the wake is more complicated. It is possible that better modeling of the wake shape will help to obtain more true values of the induced drag.

4. Conclusions

The results of the calculations show that in the calculation of the ground effect, it is necessary to take the thickness of the wing into account, when the altitude is less than the wing chord. The wing thickness changes the induced angle of attack, which changes the lift and pitching moment coefficients, and there is a little influence of the wing thickness on the gradient $dc_l/d\alpha$.

The differences between the numerical and the experimental results are the biggest in the calculations of the induced drag. However, the numerical results are in very good agreement with the results of another analytical method, based on the potential flow theory. The differences between the computed and the experimental values could appear partly due to the neglecting of the roll-up of the vortex wake.

References

1. BERTIN J., SMITH M., 1989, *Aerodynamics for Engineers,* Prentice Hall, London

2. DE SIEVERS A., Wind Tunnel Tests on the Ground Effect, *NASA TT,* F-11, 059

3. FIECKE D., 1956, *Die Bestimmung der Flugzeugpolaren für Entwurfszwecke,* Deutsche Versuchsanstalt für Luftfahrt E.V., Mülheim, Ruhr

4. HEDMAN S.G., 1965, Vortex Lattice Method for Calculation of Quasi Steady State Loadings on Thin Elastic Wings in Subsonic Flow, *The Aeronaut. Res. Inst. of Sweden,* Report 105

5. HESS J., SMITH A.M.O., 1966, Calculation of Potential Flow About Arbitrary Bodies, *Progress in Aeronautical Sciences,* 8

6. KATZ J., PLOTKIN A., 1991, *Low Speed Aerodynamics, From Wing Theory to Panel Methods,* McGraw-Hill, Inc.

7. LAN C.E., 1976, Some Applications of the Quasi Vortex-Lattice Method in Steady and Unsteady Aerodynamics, *Vortex-Lattice Utilization,* NASA SP-405

8. LIU H.T., HWANG P.A., SRNSKY R.A., 1992, Physical Modeling of Ground Effects on Vortex Wakes, *Journal of Aircraft,* **29**, 6, 1027-1034

9. MASKEW B., WOODWARD F.A., 1976, Symmetrical Singularity Model for Lifting Potential Flow Analysis, *Journal of Aircraft,* **13**, 9, 733-734

10. SINGH N., BANDYOPADHYAY G., BASU B.C., 1983, Calculation of Potential Flow About Arbitrary Three Dimensional Wings Using Internal Singularity Distributions, *The Aeronautical Quarterly,* XXXIV, 3, 197-210

11. THWAITES B., EDIT., 1960, *Incompressible Aerodynamics,* Oxford University Press

Zastosowanie metod panelowych do obliczeń charakterystyk aerodynamicznych płata z uwzględnieniem wpływu ziemi

Streszczenie

W pracy przedstawiono modele matematyczne opływu płatów w pobliżu ziemi. Założono, że przepływ jest potencjalny z wyjątkiem śladu wirowego za płatem. Szczegółowo przeanalizowano dwa modele: pierwszy dla płatów cienkich z wykorzystaniem metody siatki wirowej i drugi dla płatów grubych z wykorzystaniem metody Hessa. Obliczono globalne charakterystyki aerodynamiczne płata, w szczególności współczynniki siły nośnej, momentu pochylającego, oporu indukowanego oraz gradient siły nośnej i idukowany kąt natarcia – wszystkie w funkcji względnej wysokości płata nad pasem startowym. Przedstawiono porównanie obliczonych charakterystyk aerodynamicznych dla płatów nieskończenie cienkich oraz płatów grubych z wynikami eksperymentów.

Manuscript received June 15, 1994; accepted for print May 12, 1995